Thermal and potentiometric studies for complexes of Zr and Hf with some barbituric acid derivatives

IOP Conf. Series: Materials Science and Engineering **975** (2020) 012015 doi:10.1088/1757-899X/975/1/012015

Thermal and potentiometric studies for complexes of Zr and Hf with some barbituric acid derivatives

M S Masoud [1], A S Hassan[1], N M Desouky[1], H M kamel [2], A S El-Kholany[*2]

[1] Chemistry Department, Faculty of Science, Alexandria University, Egypt.
[2] Medical Laboratory Department, Faculty of Allied Medical Sciences, Pharos University in Alexandria, Egypt. E-mail address: elkholany73@yahoo.com

Abstract. The complexes of Barbital (Bal), Thiobarbituric acid thione (TBA), Thiobarbituric acid thiol (2-TBA), 2-Thiouracil (TU) with Zr (IV) and Hf (IV) were prepared. The structures and mode of bonding were characterized by elemental analysis, IR and electronic spectroscopy. Thermal analyses of the prepared complexes were done by DTA, TG, DSC techniques. The thermodynamic parameters were evaluated. The change of entropy values, $\Delta S^{\#}$, for all the complexes lie within the range -0.267,-0.299 KjK^{-1} mol^{-1}. The thermal processes proceed in complicated mechanisms with ordered transition states. In general, the complexes dissociated after losing small molecules such as H_2O, Cl_2 and CO. The decomposition is usually ended by the metal moiety. The DSC technique explained the effect of temperature on physical properties of some complexes. The glass transition phase doesn`t appear in all the complexes, while the crystallization temperature (Tc) was 78^0C-322.12^0C. Potentiometric titration studies calculated the dissociation constants of the ligands, the stability constants of the complexes and the distribution of species at different pH values.
Keywords. IR, DTA, TGA, DSC, Potentiometric titration, Complexes, Zr, Hf, Barbituric, Acid Derivatives.

1. Introduction

Pyrimidine ring has an important role in several biological systems, where they exist in nucleic acids, many vitamins, coenzymes, and antibiotics [1-2]. The nucleic acid is related to antimetabolites used in anticarcinogenic chemotherapy [3]. Metal complexes of pyrimidine are extensively studied for their great verity of biological activity ranging from antitumoral, antiviral, antibacterial, antimalarial, chemotherapeutic activity, etc. [4-5]. Furthermore, pyrimidines are reported as corrosion inhibitors for steel [6-7].

Barbiturates and thiobarbiturates represent important classes of medicinal compounds. Barbituric acid or 2,4,6(1H,3H,5H)-pyrimidinetrione is the lead compound of all barbiturates[1]. The synthesis of simple barbituric or thiobarbituric acids involves the condensation of malonic acid esters with thiourea or urea were used in pharmaceutical, these compounds continue to attract attention due to the wide range of biological activities. The use of compounds includes sedatives, hypnotics and antiepileptic drugs [8]. Furthermore, barbiturates and thiobarbiturates are reported to have antibacterial, antiurease and antioxidant activities[9]. In addition, some derivatives bearing the pyrimidine-2, 4, 6-trione unit have a potential therapeutic effect against diet-induced non-alcoholic fatty liver disease [10]. Some compounds include a thiobarbiturate unit that is used as inhibitors [11].The substitution on the pyrimidine-2,4,6-trione moiety is the effective pharmacophore in several different compounds

showing antitumor, anti-invasive and antiangiogenic effects [12], and also as promising compounds for amyotrophic lateral sclerosis [13]. Pyrimidine-2,4,6-triones attached to aryl hydrazones have been reported to be Ribosomal S6 Kinase 2 (RSK-2) inhibitors [14].

The thiobarbituric acid consists of a pyrimidine cyclic structure. These compounds have been described as privileged structures, as they provide various points of attachment for a diverse array of structural elements that can be used to target receptor agonists or antagonists owing to the versatile these compounds are more often used for the mankind Most of the thiobarbiturate derivatives are bilogicaly active and have many applications in agrochemicals further as pharmaceutical like herbicides, sedative, fungicidal, antiviral agents antioxidant, anti-inflammatory, antidepressant, antibacterial and antitumor, ,etc. [14-15]. The pyrimidine nucleus itself is unreactive toward electrophilic substitution reactions because of the -I and -M effects of the two nitrogen atoms while 2-thiouracil nucleus (1) is active because of the electron releasing effect of -OH and -SH groups[16-17]. Thus, 2-thiouracil could be chloro-sulphonated in a good yield [18-19].

Numerous inorganic and organometallic complexes of Zr have been described with zircon ($ZrSiO_4$), being its most widely recognized inorganic form [20-23]. Zirconium can exist in several oxidation states including (II), (III) and (IV), which is its preferred oxidation state [24]. Zirconium (II) complexes are known, but they typically require p-donor ligands to enhance stability even under inert atmosphere conditions, and even fewer reports describing the Zr (III) oxidation state exist [24].

The synthesis and characterization of a series of five heteroleptic hafnium and zirconium complexes bearing chloro ligands as well as differently substituted phenoxy benzoxazole ligands were reported [25]. All complexes had deen analyzed with regard to their structural chemistry. Moreover, their emission properties were studied, including emission spectra and excited-state lifetimes.

The original intention for this study was to introduce heavy atoms, which are in principle capable of influencing the excited state transitions as has been demonstrated earlier for so-called triplet-harvesting complexes including examples such as tris (pyridylphenyl) iridium (II) $Ir(ppy)_3$ [26], osmium(II) polypyridine complexes or a range of platinum complexes with extended heterocyclic ligands [27-29]. In our laboratory, Masoud et al reported a detailed structural chemistry, thermal and potentiometric studies of some nucleic acid complexes [30-40].

2. Experimental

2.1. General method for the preparation of the metal complexes

Ligands used are barbituric acid, barbiatal, thiobarbituric acid (thiol and thione) and 2-thiouracil, to prepare zircoium and hafnium complexes. Ligand was dissolved in hot distilled water, metal chloride was dissolved in ethanol added l with shaking for 5-7 min and a complex started to precipitate. Complexes were left 2 days to complete precipitation. The precipitated product was filtered off, washed with water and dried in vacuum at 40 °C. The analytical data are collected in table 1.

2.1.1Analysis.

a) Chloride analysis: is determined by Mohr and Volhard methods
b) N and S analysis: These are determined at the micro analytical data center at Cairo University.
c) Metal ion analysis: The metal ion contents were determined successfully gravimetrically.

2.1.2 Preparation of solutions:

a) An accurate CO_2-free 0.01 M solution of NaOH was prepared by diluting standard 1.0 M solution. The exact concentration of NaOH was determined by titrating against standard potassium hydrogen phthalate. Standard NaOH solution was analyzed from time to time. The solution was preserved in a waxed bottle fitted with a $CaCl_2$ tube.
b) 0.1 M solution of KCI was prepared to adjust the ionic strength of solutions.

2.2. Instruments and procedures:

2.2.1. Infrared spectra.

The KBr disc infrared spectra of the ligands and their metal complexes are measured over the frequency range 500-4000 cm^{-1} using BRUKER TENSOR 37 FT-IR spectrophotometer. Calibration of frequency readings is made with polystyrene film (1602±1 cm^{-1}).

Table 1. Analytical data of the prepared complexes

Complex	Reaction	N		S		Metal		Cl	
		Calc.	Found	Calc.	Found	Calc.	Found	Calc.	Found
HfCl.2Bal	$HfCl_4$ + Bal(1:1)	9.6	10.1	---	---	30.6	30.6	6.1	6.9
ZrCl.Bal	$ZrCl_4$ + Bal(1:1)	9.0	9.6	---	---	29.3	30.1	11.4	11.5
$[Hf.TU.H_2O]Cl_2$	$HfCl_4$ + TU(1:1)	7.1	7. 5	8.1	8.5	---	---	17.9	17.7
$[Zr.TU.H_2O]Cl_3$	$ZrCl_4$ + TU(1:1)	8.1	8.3	9.3	9.7	26.5	26.6	31.0	31.1
$[Hf.BA.H_2O]Cl_2$	$HfCl_4$ + BA(1:1)	7.1	7.3	---	---	45.1	45.2	17.9	17.7
ZrCl.2BA	$ZrCl_4$ + BA(1:1)	14.6	15.1	---	---	23.8	24.1	9.2	9.4
$HfCl_2.2BACl_2$	$HfCl_4$ + BA(1:2)	14.7	15.1	---	---	23.4	24.2	9.3	9.5
$[ZrCl.2BA.H_2O]Cl$	$ZrCl_4$ + BA(1:2)	14.9	15.2	---	---	16.1	16.5	12.6	12.6
$[Hf.2TU.2H_2O]Cl_2$	$HfCl_4$ + TU(1:2)	10.2	10.8	11.4	11.7	31.5	31.7	12.7	12.6
$[ZrCl_4.2TU]3H_2O$	$ZrCl_4$ + TU(1:2)	6.7	7.1	7.7	7.8	21.9	22.5	34.2	34.9
[Hf.2TBA]Cl	$HfCl_4$ + TBA(1:2)	11. 2	11.3	12.8	12.9	35.5	36.6	7.0	6.2
$ZrCl_4.2TBA$	$ZrCl_4$ + TBA(1:2)	7.4	7.6	8.5	9.1	24.1	24.4	37.7	38.4
HfCl.2(2-TBA)	$HfCl_4$ + 2-TBA(1:2)	11.2	11.7	12.8	13.1	35.5	35.7	7.0	6.7
[Zr.2(2-TBA)]Cl	$ZrCl_4$ + 2-TBA(1:2)	13.5	13. 6	15.4	15.7	21.9	22.1	8.6	8.9

2.2.2 Thermal analysis.
Differential thermal analysis (DTA), the thermo-gravimetric analysis (TGA) and differential scanning calorimetry (DSC) are carried out for some complexes using SEIS STA PT 1000 at the micro analytical data center at Cairo University, Egypt. The rate of heating was 10°C/min.

2.2.3. Potentiometric measurements.
These were carried out using a Jenway-3505 pH-meter. The electrode system was calibrated before and after each serious of pH measurements under the same conditions using standard buffers of pH`s 4.0, 7.0 and 10. The titration cell consisted of water jacketed 150 ml vessel fitted with a polyethylene stopper in which appropriately located holes are present, one of them allowed the insertion of a micro-burette containing CO_2 free NaOH.

Another hole was used to insert the electrode. Also there are holes for the inlet and outlet of the nitrogen gas that was purified as follows: it was passed through a train of bubbles containing successively silver nitrate to get rid of any traces of oxygen, followed by copper sulphate solution and alkaline pyrogallol to get rid of the oxygen too. The gas was passed through a tube containing $CaCl_2$ to get rid of moisture and CO_2.

The potentiometric titration procedure to evaluate the dissociation constants of the organic compounds was carried out by introducing the appropriate volume of the organic compound into the titration cell followed by 5 ml KCl solution of an ionic strength 0.1 M, and completed to 50 ml with doubly distilled water. Before each titration the solution in the titration vessel was left for about 15 min to attain the desired constant temperature (25°C) which is controlled by using a thermostatic device. During the whole titration, purified nitrogen gas was slowly bubbled in the solution.

The same potentiometric titration experiments were applied for studying the complexes equilibria in 75%, 50% and 25% (V/V) ethanol-water. This was constructed as follows, the complex solution {2 ml 10^{-3} M metal chloride + 5 ml 10^{-3} M ligand + 5 ml 0.1 M KCI + (29, 19 and 9 ml) ethanol and completed to 50 ml by distilled water} was titrated against standard NaOH. The experiments were done using the same conditions of titrating the organic compounds.

Correction of the pH-readings with a correction term δ for mixed solvents (ethanol-water) calculated by the following equation: ($\delta = pH_x - pH_S$) Where pH_x and pH_s are the values of unknown and standard buffer solutions, δ = 0.28 for 25% (ethanol - water), δ= 0.35 for 50% (ethanol - water) and δ=0.45 for 75% (ethanol- water) [41].

3. Results and discussion

3.1. Infrared spectra

3.1.1. Infrared spectra of the Iigands.

The IR spectra of solid BA, TBA, 2-TBA, TU and Bal are aimed to be investigated to determine the assignment of the vibrational frequencies especially of the fundamental groups (C-O, N-H, C=S and OH), table 2. This facilitates the tracing of keto-enol tautomerism phenomena.

The ring in BA is significantly distorted from planarity; the methylene part of the ring has a boat configuration [42]. Thus, the symmetry of the isolated molecule is C_5 of C_{2V}. The latter is not possible in the solid because of the manner in which the molecules are linked by hydrogen bonds.

The solid BA contains pairs of molecules linked through two hydrogen bond bands, between the N-H groups in the 3 positions and carbonyls in the 2 position are in a ribbon structure through hydrogen bonds between the N-H groups in 1 position and carbonyls in the 4 position. The carbonyl in the 6 position is not involved in the hydrogen bonding [43-46]

TBA is a heterocyclic compound containing thioamide group -NH-C=S) can exist in either the thione (TBA) or the thiol (2-TBA) form [47]. In general, the protropic tautomers of hetero aromatic compounds comprise a mobile hydrogen atom to be moved from one site to another.

For TBA, the absence of ν S-H stretching at 2500 cm^{-1} and the presence of an absorption at 1546 cm^{-1} due to ν C-N suggests the thione (A) tautomer is more predominated in the solid rather than the thiol (B):

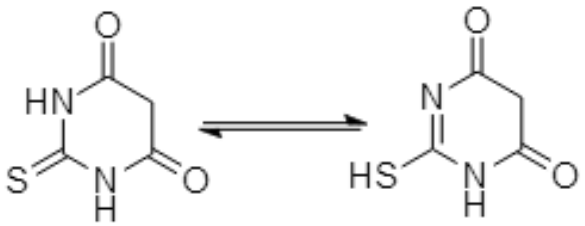

The strong band at 1297.9 cm^{-1} is due to δ O-H, the ν C=S and ν C-N are identified by the presence of strong bands at 1242.8 and 1163.7 cm^{-1} which refer to the existence of the following tautomers:

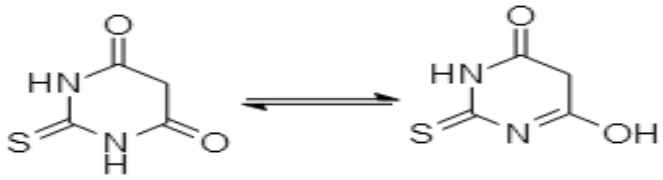

For (TBA), the disappearance of a well-defined bands at the range 3565-3450 cm^{-1} of a hydrogen bond of the type N-H.....O and appearance of a broad band at 3564.50 cm^{-1} of O-H type is an evidence of the existence of 2-thiobarbituric acid. The appearance of νS-H stretching at 2596.27 cm^{-1} and the band at 1567.53 cm^{-1} due to νC=N suggests the thiol tautomer.

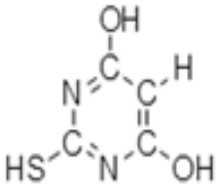

The vibrational spectrum for (TU) has been interpreted assuming planar geometry and C_s point group symmetry. The oxygen atom attached to C_4 takes part in the hydrogen-bonding of the type N-H....O, the S-atom does not participate in the hydrogen- bonding.

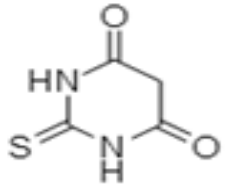

The presence of well-defined splitting three bands of stretching vibrations for barbital of the NH groups are present in the frequency range 3080.91- 3210 cm^{-1} and three CH stretching modes associated with the ethyl groups is located at the range 2984.43-2866.91 cm^{-1}

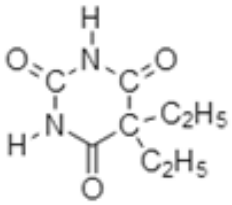

3.1.2. Infrared spectra of the prepared metal complexes.

It is necessary to investigate the infrared spectra of the complexes compared to that of the free ligand, Table (2), Figures (1-5) In general, the metal complexation may increase or decrease the vibrational frequency of the coordinated functional group depending on the strength of π-interaction occurring between the metal ion and the π-electron of the functional groups.

IR spectra suggest the participation of nitrogen and oxygen atoms on complexation. For $[Hf.BA.H_2O]Cl_2$ complex, the bands at 1413 and 1233 cm^{-1} are red shifted which represent C-N stretches and the bands at 3187-3099 cm^{-1} which represent NH groups symmetric and asymmetric vibrations are disappeared and the band at 1717 cm^{-1} is red shifted which suggest the contribution of the oxygen atoms on complexation, a very broad band at 3408 cm^{-1} has appeared which may represent the contribution of H_2O on complexation and/or hydrogen bonding. The 2Cl atoms are in the outer coordination sphere.

For $HfCl_2.4BA$ and $[ZrCl.3BA.H_2O)CI$ complexes, the atom band on at 3099 cm^{-1} is disappeared indicating the contribution of one nitrogen atom on complexation. The bands at 1619, 1413 and 1233 cm^{-1} are blue shifted slightly for ZrCl.2BA and $HfCl_2.4BA$ complexes confirming the nitrogen atom involvement on complexation. For $[ZrCL.3BA.H_2O]CI$ complex, the band at 3562 cm^{-1} is red shifted by 30 cm^{-1} which may indicate H_2O is involved on complexation and/ or existence of hydrogen bonds. The strong band at 1717 cm^{-1} in the free ligand assigned as C=O becomes of different shapes on complexation, i.e. still exists at 1717 cm^{-1} in a strong feature in $[ZrCl.3BA.H_2O]Cl$ complex and in ZrCl.2BA and $HfCl_2.4BA$ complexes in a broad feature. Cl atoms of $[Zr.3BA.H_2O]Cl_2$ complex are outer and inner the coordination sphere, but for ZrCl.2BA and $HfCl_2.4BA$ complexes are in the inner sphere.

The $[Hf.TU.H_2O]Cl_2$, $[Zr.TU.H_2O]Cl_3$ and $[Hf.2TU.3H_2O]Cl_2$ complexes, gave IR bands at 1422 and 1564 cm^{-1} are blue and red shifted, respectively, which imply that nitrogen atom is contributed on complexation, the band at 1701 cm^{-1} is blue and red shifted which indicated the involvement of the oxygen atom on complexation. The band at 1213 cm^{-1} which represents C=S is red shifted to suggest the contribution of the sulphur atom on complexation. All Cl atoms are in the outer coordination sphere.

For $[ZrCl_4.TU].3H_2O$ complex showed a very broad band at 3421.45 cm^{-1} which may represent the contribution of H_2O on complexation and/ or hydrogen bonding. The band at 1422 cm^{-1} is red shifted which indicates that the nitrogen atom is contributed on complexation, the band at 1701 cm^{-1} is blue shifted and may refer to the involvement of the oxygen atom on complexation.

The band at 3450 cm^{-1} is strongly red shifted by ~40 cm^{-1} for [Hf.2TBA]CI and $ZrCl_4$.TBA complexes, the band at 1163 cm^{-1} is blue shifted indicating the nitrogen atom contribution on complexation. The band at 1646 cm^{-1} (the average band at 1693, 1643 and 1603 cm^{-1}) is red shifted which suggests the involvement of the oxygen atom in complexes, the band at 1443 cm^{-1} is disappeared. Furthermore, for [Hf.2TBA]Cl complex the band at 1242 cm^{-1} is disappeared and the band at 3104 cm^{-1} is blue shifted, for $ZrCl_4$.TBA complex the band at 1242 cm^{-1} is red shifted and the band at 3186 cm^{-1} is disappeared.

The band at 3099 cm^{-1} is blue shifted for HfCl.2(2-TBA) and [Zr.2(2-TBA)]Cl complexes. The band at 1162 cm^{-1} is blue shifted indicating the nitrogen atom contribution on complexation. The band at 3565 cm^{-1} is strongly red shifted by ~170 cm^{-1} for the complexes and the band at 1663 cm^{-1} (the average band at 1720, 1650 and 1618 cm^{-1}) is strongly red shifted for HfCl.2(2-TBA) complex and blue shifted for [Zr.2(2-TBA)]CI complex to suggest the involvement of the oxygen atom in complexes. The band at 1437 cm^{-1} is red shifted. Furthermore, for HfCl.2(2-TBA) complex the band at1239 cm^{-1} is disappeared.

IR spectra suggest the participation of nitrogen and oxygen atoms on complexation. For HfCl.2Bal complex, the band at 1461 cm^{-1} is blue shifted representing C-N stretches and the bands at 3210- 3081 cm^{-1} representing NH groups symmetric and asymmetric vibrations are changed in their shape and red shifted by ~ 40 cm^{-1}. The bands at 1766 and 1719 cm^{-1} are blue shifted and the band at 1679 cm^{-1} is red shifted which suggest the contribution of the oxygen atoms on complexation. The Cl atom is in the inner coordination sphere.

For ZrCl.Bal complex, the band at 1461 cm^{-1} in Bal is red shifted representing C-N stretches, the bands at 1766 and 1719 cm^{-1} are blue shifted and the band at 1679 cm^{-1} is red shifted which refers to the contribution of the oxygen atoms on complexation. The Cl atom is in the inner coordination sphere. This complex gives very weak changes in IR spectra.

Table 2. Some fundamental Infrared bands

compound	νO-H	νN-H	νS-H	νC-H	νC=O	νC=N	νC-N	νC=S
BA	3562, 3477	3187, 3099	-----	2878	1749, 1717	1619	1413, 1233 1192	------
[Hf.BA.H_2O]Cl_2	3409	-------	-------	-------	1622	-------	1360, 1292	-------
ZrCl.2BA	3562, 3478	3188, 3099	-------	2877	1750, 1717	1622	1416, 1236 1193	-------
$HfCl_2$. 4BA	3562, 3478	3189	-------	2877	1717	1622	1416, 1236 1193	-------
[ZrCl.3BA.H_2O]Cl	3533, 3477	3188	-------	2880	1749, 1718	1620	1414, 1234 1193	-------
Bal	-------	3210, 3166 3081	-----	2984, 2943 2867	1766, 1719 1679	-----	1460, 1324 1241	------
HfCl.2Bal	-------	3249, 3087	-------	2973, 2946 2878	1769, 1722 1676	-------	1463, 1324 1238	-------
ZrCl.Bal	-------	3210, 3167 3080	-------	2985, 2945 2865	1767, 1720 1678	-------	1460, 1324 1240	-------
TBA	3565, 3450	3187, 3105	-----	2920, 2877	1693, 1643 1604	1546	1164	1443 1242
[Hf.2TBA]Cl	3408	3189, 3110	-------	2887	1630	-------	1186	-------
$ZrCl_4$.TBA	3601, 3411	3104	-------	2880	1626	-------	1190	1226
2-TBA	3565	3099	2596	2872	1720, 1650 1618	1568	1162	1437 1239
HfCl.2(2-TBA)	3383	3103	-------	2874	1618	-------	1165	1406
[Zr.2(2-TBA)]Cl	3396	3101	2598	2873	1721, 1651 1619	1568	1163	1431 1239
TU	3490	3084, 3047	------	2926	1701	1565	1423	1213
[Hf.TU.H_2O]Cl_2	3463	3084, 3047	-------	2928	1705	1563	1421	1212
[Zr.TU.H_2O]Cl_3	3484	3082, 3046	-------	2926	1699	1562	1421	1210
[Hf.2TU.3H_2O]Cl_2	3485	3081, 3044	-------	2924	1696	1562	1419	1210
[$ZrCl_4$.TU]3H_2O	3421	3086	-------	2930	1705	1564	1421	1213

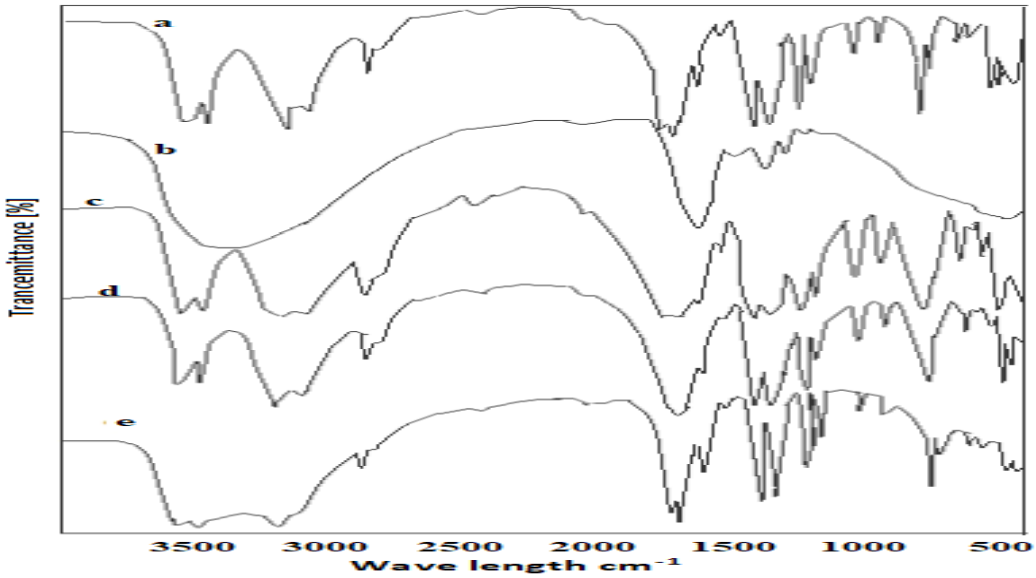

Figure 1. Infra-Red spectra of Barbituric acid (BA) and its complexes
a)BA b) $[Hf.BA.H_2O]Cl_2$ c) HfCl2. 4BA
d) ZrCl.2BA e) $[ZrCl.3BA.H_2O]Cl$

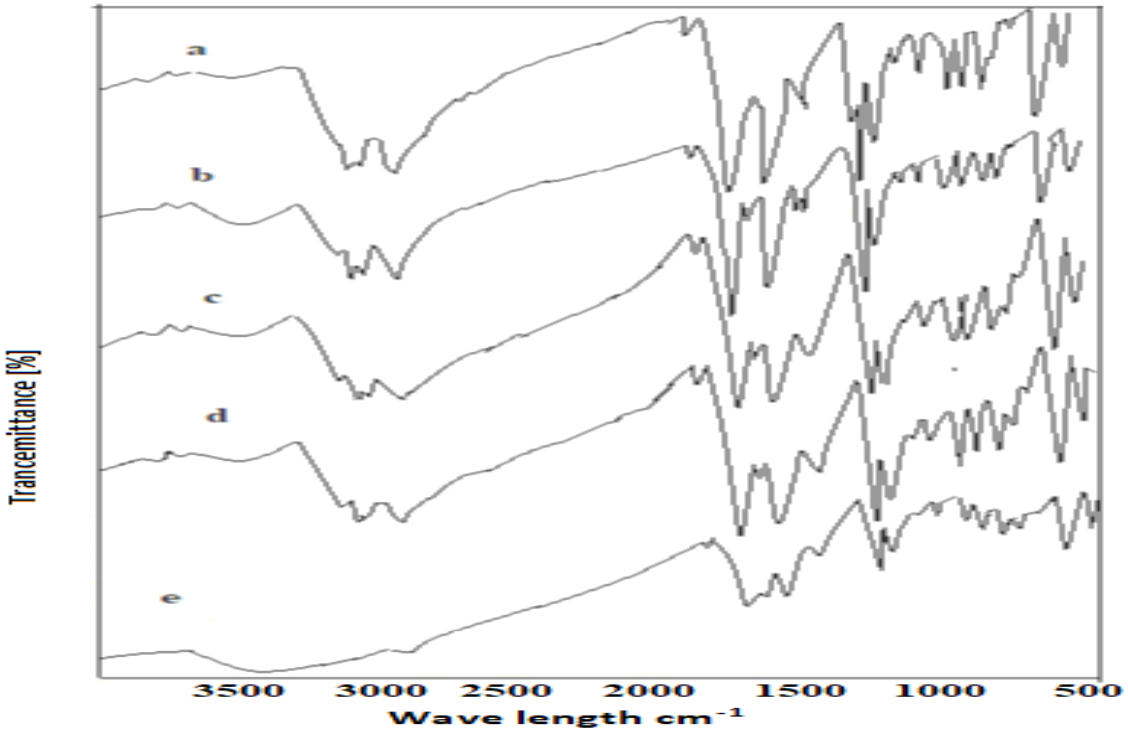

Figure 2. Infra-Red spectra of Thiouracil (TU) and its complexes:
a)TU b) $[Hf.TU.H_2O]Cl_2$ c) $[Hf.2TU.3H_2O]Cl_2$
d) $[Zr.TU.H_2O]Cl_3$ e) $[ZrCl_4.TU]3H_2O$

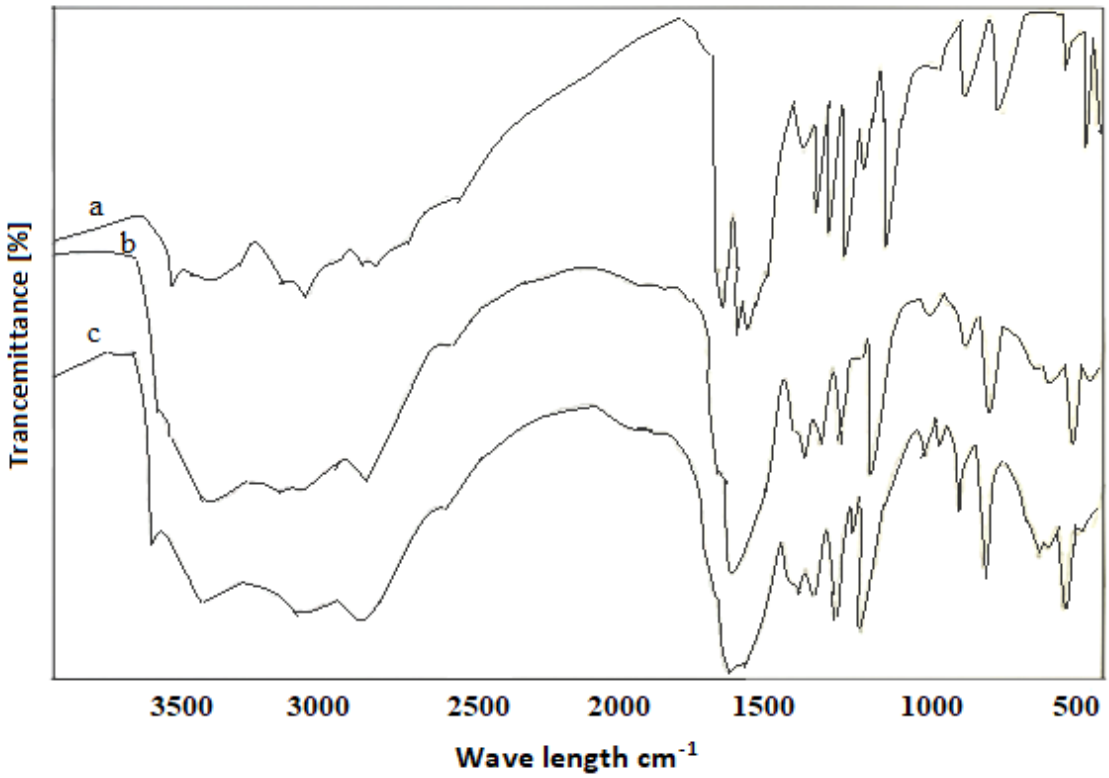

Figure 3. Infra-Red spectra of Thio barbituric acid(TBA) and its complexes:
a)TBA b) [Hf.2TBA]Cl c) $ZrCl_4$.TBA

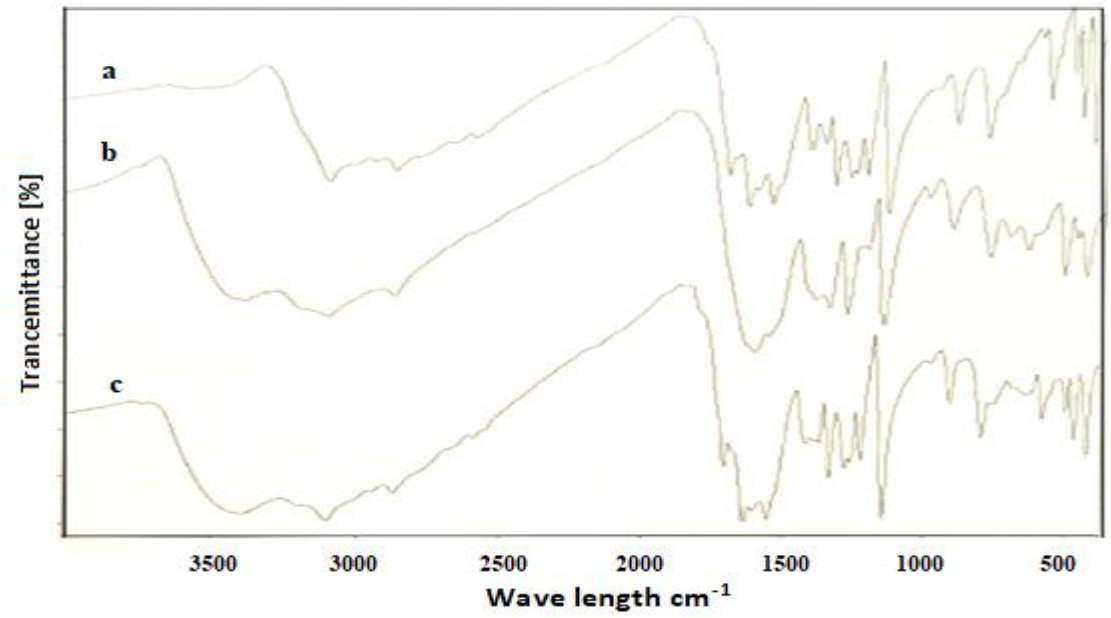

Figure 4. Infra-Red spectra of 2-Thio barbituric acid(2TBA) and its complexes
a) 2-TBA b) HfCl.2(2-TBA) c) [Zr.2(2-TBA)]Cl

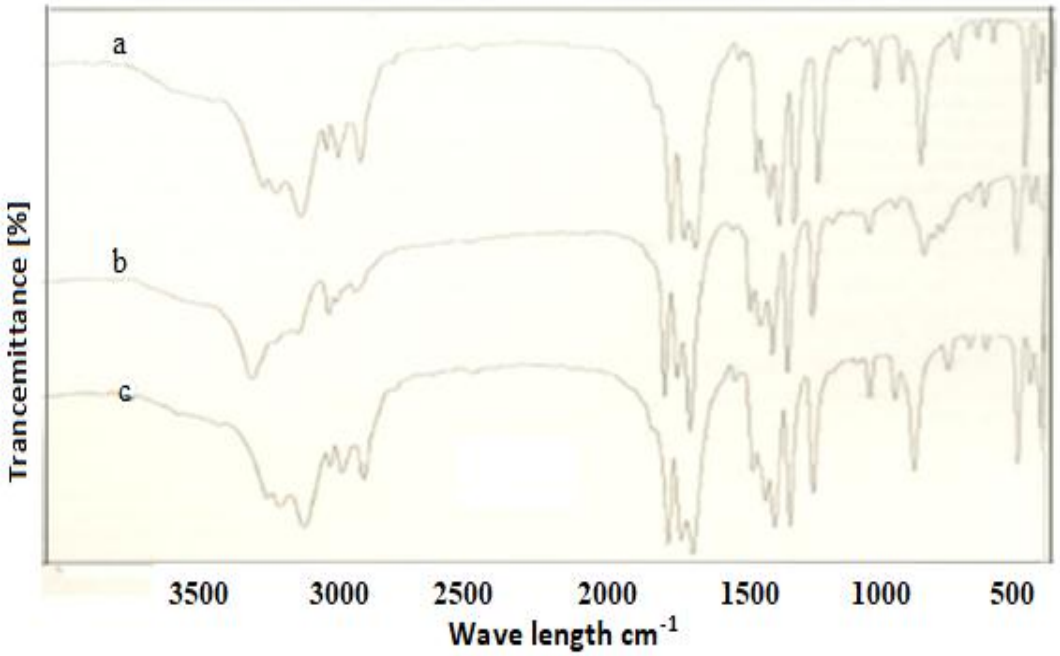

Figure 5. Infra-Red spectra of Barbital (Bal) and its complexes:
a)Bal b) HfCl.2Bal c) ZrCl.Bal

3.2. Thermal analysis
3.2.1 DTA and TGA.
The order of the reaction process (first-order, second-order, .. etc.) will be determined from the symmetry of the DTA curve. The asymmetry of the peak is simply a/b and also the reaction order is calculated as follows:

$$S = 0.63\ n^2 \quad \text{and} \quad n = 1.26\ (a/b)^{1/2} \tag{1}$$

The values of collision factor, Z, is obtained in case of Horowitz
Metzger from the relation

$$z = \frac{\Delta E_a}{R T_m} \beta \exp\left(\frac{\Delta E_a}{R T_m^2}\right) \tag{2}$$

Also, the entropies of activation ($\Delta S^{\#}$) can be obtained from the relation:

$$z = \frac{k T_m}{h} \exp\left(\frac{\Delta S^*}{R}\right) \tag{3}$$

Where, R represents molar gas constant, β rate of heating (KS^{-1}), k is the Boltzmann constant and h is the Planck's constant.
From the DTA curves the heat of transformation, $\Delta H^{\#}$, could be calculated. For any phase transformation taking place at any peak temperature, T_m, the change in enthalpy ($\Delta H^{\#}$) is obtained from the following equation:

$$\Delta S^{\#} = \Delta H^{\#} / T_m \tag{4}$$

Thermal studies (DTA, TGA and DSC) were carried out for some of the prepared complexes (Zr and Hf), table 3, representative example for [ZrCl.3BA.H_2O]CI complex is given in figures 6 and 7.

The decomposition of the complex occurred in three steps. The first step started at 51.30 °C - 141.88 °C where the % loss was found to be 6.063% (calculated 6.317%) attributed to the loss of Cl atom in the outer sphere. In the second step between 141.88 °C - 304.16 °C, % loss of 76.852% was obtained due to fragmentation of H_2O and three barbituric moieties. The last step at 367.50°C - 513.07 °C is due to the loss of the second Cl atom leaving a residue of Zr moiety. The following scheme for the decomposition is suggested:

$$[ZrCl(3BA)H_2O]\,Cl \xrightarrow[51^oC - 142^oC]{-\,Cl} [ZrCl(3BA)H_2O] \xrightarrow[142^oC - 304^oC]{-\,(3BA)H_2O} ZrCl \xrightarrow[368^oC - 513^oC]{-\,Cl} Zr$$

The DTA show two endothermic peaks with T_m = 74.45-118.37 °C. Two other endothermic peaks were obtained with T_m = 250.85 °C and 274.74°C attributed to the decomposition of the complex leaving Zr moiety as residue.

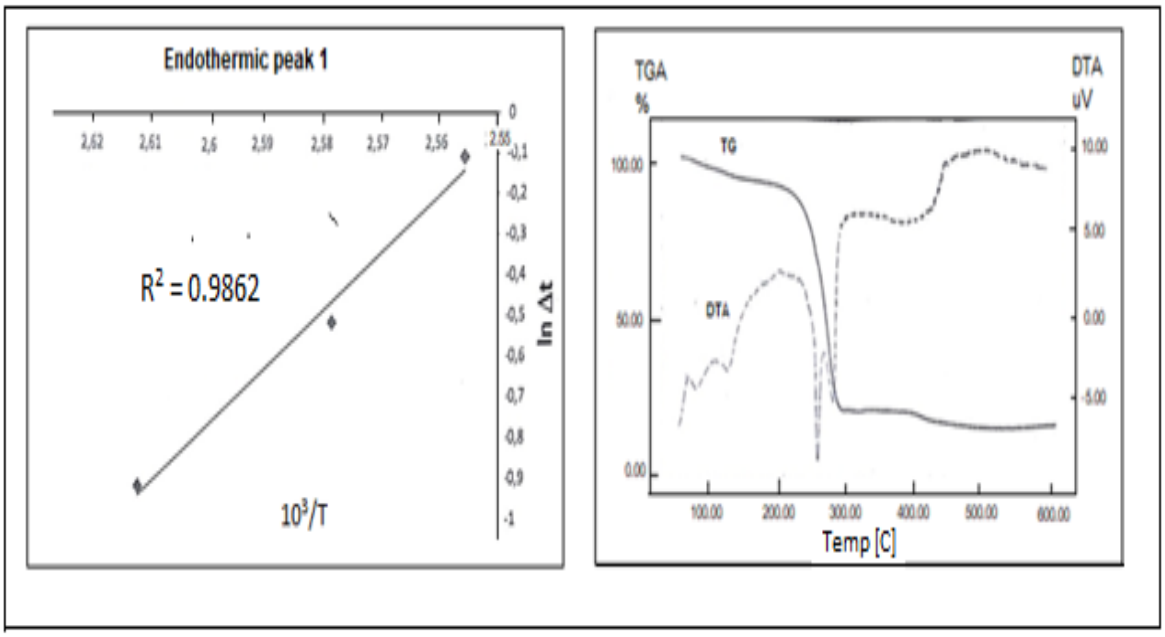

Figure 6. TG & DTA curves of [ZrCl.3BA.H_2O]CI complex

The TG and DTA curve of [Hf.2TBA]Cl complex, the decomposition occurred in three steps. The first step started at 42.15 °C-104.31 °C where the % loss was found to be 8.593% (calculated 7.121%) attributed to the loss of Cl atom in the outer sphere. In the second step between 104.31°C- 274.07°C, % loss of 31.254% (calculated 31.896%) was obtained due to fragmentation of one TBA moiety and O atom from the second ligand. The last step at 274.07°C-585.93°C is due to the loss of 2-TU leaving a residue of Hf moiety, (found 26.545%, calculated 25.276%).

The TG and DTA curves of HfCl.2(2-TBA) complex, it is clear that the complex showed a multistage mechanism. A step between 32.78 °C- 137.52 °C is due to the loss of CO molecule with % loss of (found 5.817%, calculated 5.6179%). The second step between 137.52°C-248.12°C is attributed to the loss of H_2O molecule and Cl atom (found I1.729%, calculated 10.732%). The third

step between 248.12°C 404.81°C with a weight loss of found 19.855%, (calculated 20.060%) is due to the fragmentation of $C_3H_3N_2S$. The last step between 404.81°C-601.44°C, % weight loss of found 23.237%, (calculated 22.111%) is due to the loss of the rest of the complex ending with the formation of HfO_2.

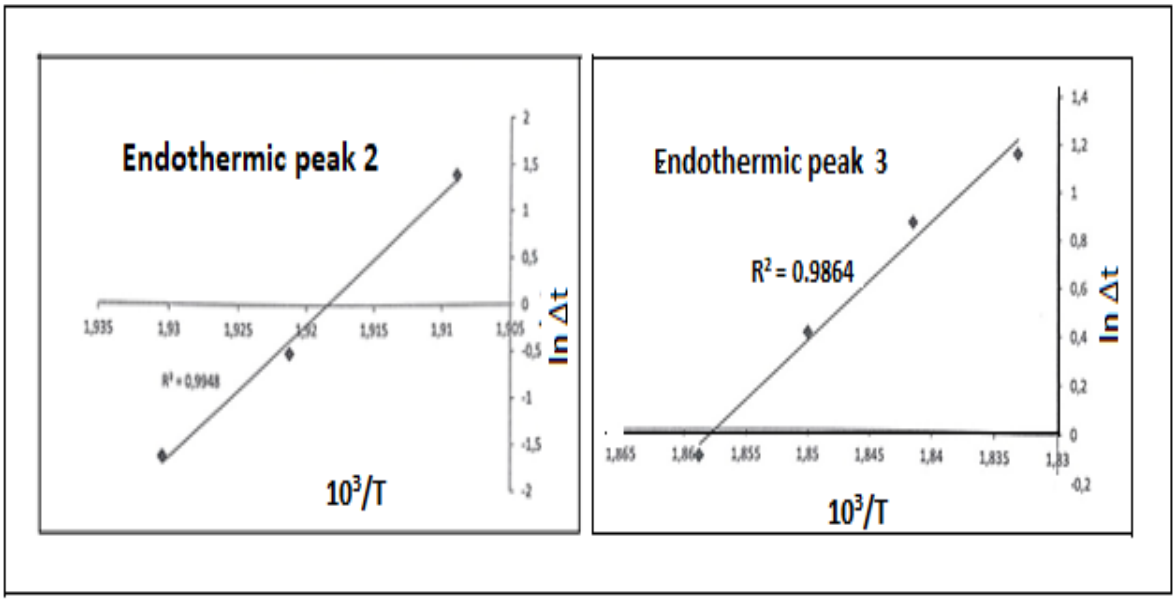

Figure 7. Plot constructed from DTA curves of [ZrCl.3BA.H_2O]CI complex

The TG and DTA curves of [Zr.2(2-TBA)]Cl complex is decomposed in a multistep form. The first step between 23.93°C - 134.80°C with % loss of (found 12.204%, calculated 12.758%) due to the loss of Cl atom in the outer sphere and O atom decomposed from one of the two ligands. The second step between 134.80°C - 273.39°C is assigned to the loss of one 2-TBA (found 34.324%, calculated 34.508%). The third step between 273.39 °C - 568.94°C is due to the loss of 2-TU leaving a residue of Zr atom moiety, (found 33.483%, calculated 30.620%).

Table 3. The DTA analysis data of the complexes

Complex	Type	a	b	Slope	T_m °K	ΔE_a (KJ mol^{-1})	n	α_m	$\Delta S^{\#}$ KJ K^{-1} mol^{-1})	$\Delta H^{\#}$ (KJ mol^{-1})	10^3Z (Sec^{-1})
[ZrCl.3BA.H_2O]Cl	Endo	1.4	0.9	-14.32	118.37	119.07	1.57	0.55	-0.27	-32.43	0.121
	Endo	0.7	0.6	-139.77	250.85	1162.08	1.36	0.57	-0.27	-67.11	0.555
	Endo	1.4	2.1	-50.22	274.74	417.49	1.03	0.63	-0.28	-76.25	0.183
[Hf.2TBA]Cl	Endo	0.7	1.1	-20.98	242.36	174.45	1.01	0.63	-0.28	-68.51	0.087
	Endo	1.2	0.7	-53.53	418.77	445.01	1.65	0.54	-0.28	-118.93	0.128
	Exo	2.4	2.1	-13.50	533.13	112.23	1.35	0.58	-0.30	-159.65	0.025
		2.4	2.1	-56.02	533.13	465.73	1.35	0.58	-0.29	-153.34	0.105
[$ZrCl_4$.TU]3H_2O	Endo	1.0	2.5	-17.21	310.95	143.10	0.80	0.67	-0.29	-89.70	0.055
HfCl.2(2-TBA)	Endo	1.2	0.6	-16.65	310.78	138.41	1.78	0.52	-0.29	-89.74	0.054
		1.2	0.6	-72.80	310.78	605.24	1.78	0.52	-0.28	-85.93	0.234
	Exo	2.1	2.0	-16.27	536.58	135.24	1.29	0.58	-0.30	-159.91	0.030
		2.1	2.0	-56.78	536.58	472.05	1.29	0.58	-0.29	-154.33	0.106
[Zr.2(2-TBA)]Cl	Endo	1.0	1.0	-42.40	251.40	352.51	1.26	0.59	-0.28	-69.75	0.168
	Exo	0.3	1.9	-93.70	482.58	779.05	0.50	0.75	-0.28	-135.94	0.194
		0.3	1.9	44.93	482.58	-373.51	0.50	0.75	-------	---------	-0.093
	Exo	2.6	1.3	-41.97	516.65	348.92	1.78	0.52	-0.29	-149.57	0.081

For the DTA of this complex, an endothermic peak with T_m= 251.40°C was obtained due to the loss of one of the two ligands and two exothermic peaks were obtained with T_m=482.58°C and T_m=516.65°C respectively. The first exothermic peak occurred with phase transition and the second exothermic peak is broad, verifying the decomposition of the complex in a multistep form.

The TG and DTA curves of [$ZrCl_4$.TU].3H_2O complex, the decomposition occurred in two steps. The first step started at 37.88°C-179.75°C where the % loss was found to be 6.064% attributed to the loss of 3H_2O molecules from the outer sphere. In the second step between 179.75°C-373.23°C, % loss of 82.88% is due to the loss of the rest of the complex leaving a residue of Zr moiety.

3.2.2 Differential scanning calorimetry (DSC)

DSC curves and physical properties obtained for the complexes are presented in figures 8-10 and table 4 and 5. The glass transition phase does not appear in all of the complexes studied. Above the glass transition, the samples have a lot of mobility. When they reach the correct temperature, they gain enough energy to convert to very ordered arrangements, i.e. crystals. When samples fall into these crystalline arrangements, they give off heat. However, this drop in the heat flows as a big dip in the plot of heat flow versus temperature. The temperature at the lowest point of the dip represents the samples crystallization temperature. Measuring the area of the dip, gives the latent energy of crystallization for the samples. Since samples give off heat when it crystallizes, crystallization is an exothermic transition.

The crystallization temperatures (T_c) of the complexes studied were around 78°C-322.12°C. All metal complexes measured have two crystallization temperatures except of [$ZrCl_4$.TU].3H_2O complex has one crystallization temperature. The heat flow is shown in units of heat (g) supplied per unit time (0). The heating rate is temperature increase (T) per unit time (t).

Heat capacity (C_p) can be determined by dividing the heat flow (q/t) by the heating rate (T/t). That is to say, heat supplied divided by the temperature increase. It is the heat absorbed by a closed system of constant composition on raising the temperature 1K.

The variation of C_p versus T can be represented using Debye model as the following relations: Where "a" is the slope of the line and "b" is the intersection of the line with y-axis (C_p axis). C_p is the specific heat at constant volume (γ) a constant equals 10-4 (cal/gram.mole.K^2).

By plotting C_p/T as y-axis and T^2 as x-axis, figure 9, a straight line with a slope equals α and the intersection with y-axis gives the coefficient (γ) is obtained, hence the Debye temperature can be determined.

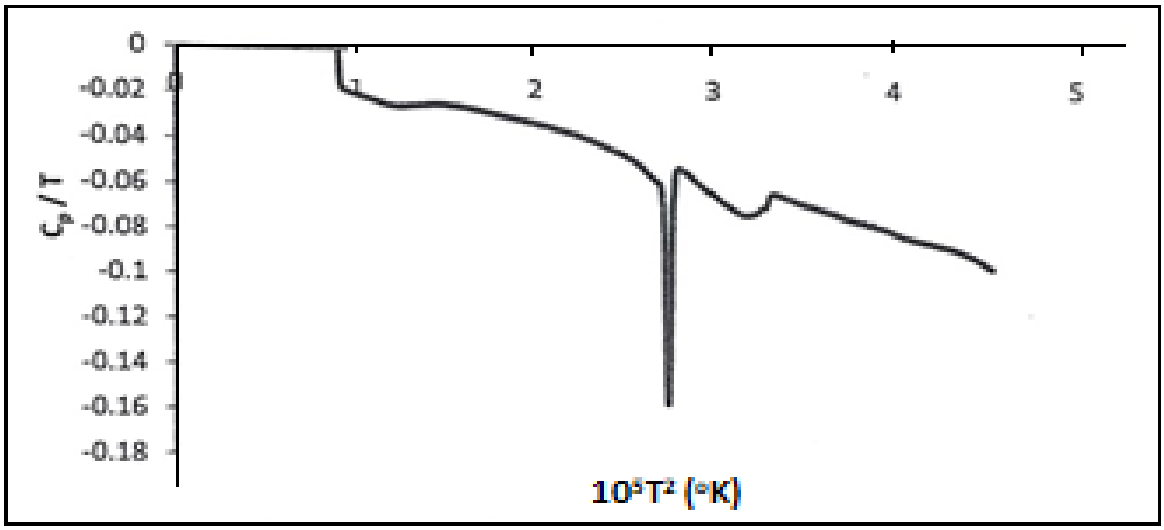

Figure 8. DSC curve for [ZrCl.3BA.H_2O]CI complex

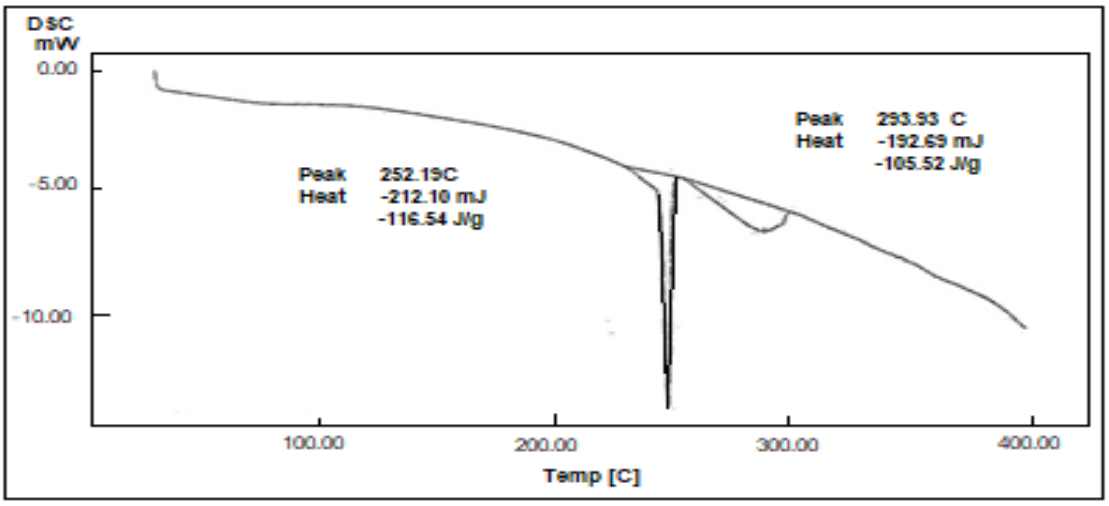

Figure 9. DSC curve C_p/T vs. T^2 for [ZrCl.3BA.H_2O]CI complex

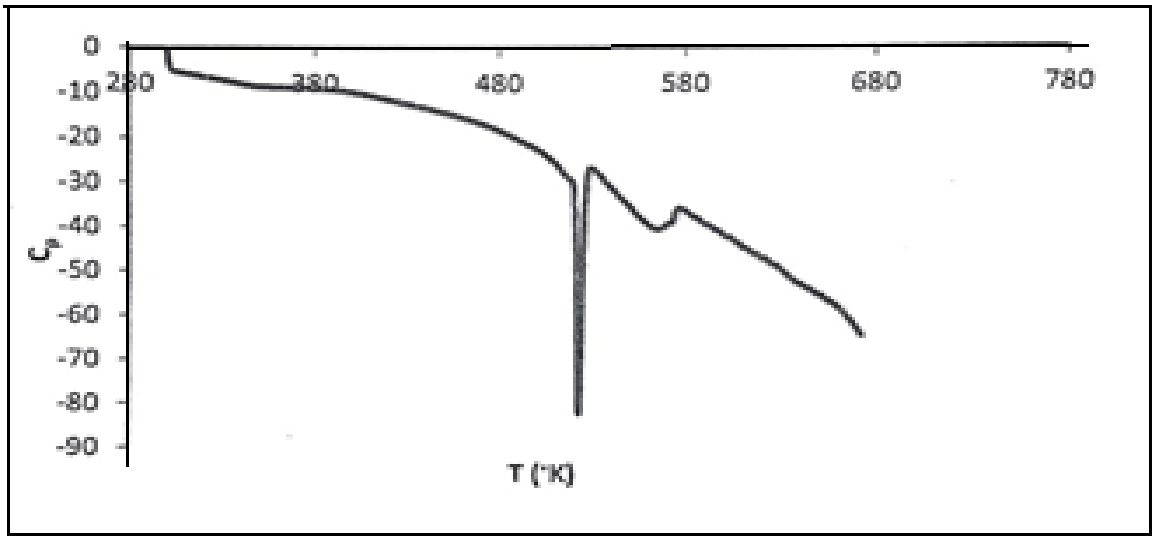

Figure 10. Dependence of C_p on T for [ZrCl.3BA.H_2O]CI complex

Table 4. Crystallization temperature of the complexes

Complex	Crystallization temperature (T_c) (°C)
[ZrCl.3BA.H_2O]Cl	252.19, 293.93
[$ZrCl_4$.TU].3H_2O	322.12
[Hf.2TBA]Cl	78.21, 242.69
HfCl.2(2-TBA)	80.82, 315.83
[Zr.2(2-TBA)]Cl	210.79, 241.84

Table 5. Variation of a, b, α and γ for the complexes according to Debye model

Complex	$C_p = aT + b$		$C_p/T = \alpha T^2 + \gamma$	
	a	b	α x 10^{-7}	γ
[ZrCl.3BA.H_2O]Cl	-0.0760	17.806	-2	0.0049
	-0.0207	-1.271	-6	0.1216
	-0.1166	37.922	-2	0.0205
	-0.4288	201.01		
	-0.2558	112.32		
[$ZrCl_4$.TU]3H_2O	-0.1065	26.866	-2	0.0096
	-0.1369	48.097	20	-0.7650
	1.2223	-792.60		
[Hf.2TBA]Cl	-0.2949	85.897	-10	0.1001
	-0.0608	13.103	-1	-0.0094
	-0.3063	130.64	-3	0.0274
	-0.1912	80.906	-2	0.0191
HfCl.2(2-TBA)	-0.1655	4.5050	-7	0.5170
	-0.0618	14.981	-1	-0.0082
	-0.1555	57.914	-3	0.0239
	-0.1549	59.584	-2	0.0115
	-0.4247	210.90	-6	0.1290
	0.1229	-109.14	2	-0.1454
	-0.2979	159.07	-3	0.0716
[Zr.2(2-TBA)]Cl	-0.1400	35.611	-5	0.0208
	0.0130	-19.180	2	-0.0626
	-0.0629	11.497	-0.7	-0.0239
	-0.6771	317.13	-10	0.2135
	-0.2169	91.859	-2	0.0154
	-0.3347	172.43	-3	0.0369

3.3. Potentiometric titration studies

The potentiometric studies in this work are divided into two parts as follows:

(1) Experiments for the free ligands in presence of 25%, 50% and 75% (v/v) of ethanol-water media at 25°C.

(2) Experiments of the complex solutions in presence of 25%, 50% and 75% (v/v) in ethanol-water media at 25°C.

3.3.1. Potentiometric studies of the free ligands in presence of different percentages of ethanol-water media.

Acid-base titration techniques were used to determine the acidity and stability constants. The Potentiometric measurements depends on the determination of the average number of the protons related to the reagent, $\overline{n}_A$. This was resolved at different pH's using the simplified following equation [48]

$$\overline{n}_A = Y - \frac{V_i N^\circ}{V_\circ C_A} \quad (5)$$

Where, V_i refers to the volume of alkali needed to achieve a given pH on the titration curve, Vo is that the initial volume of the ligand, N° is that the alkali concentration, C_A is that the total concentration of

the ligand and Y is that the number of replaceable hydrogen atoms in the ligand. The dissociation constants have been obtained by plotting $\overline{n}_A$ versus pH for the free ligands. One pK's value has been obtained for ligands with Y=1 by recording the pH values at $\overline{n}_A$ = 0.5 [49]. Where similar results have been obtained; the data were collected in table 6.

Table 6. pK values for the ligands in Ethanol-water media at 25°C (KCl =0.1M).

Ligand	$\overline{n}_A$ - pH			Point-wise method			Algeberic method		
	75%	50%	25%	75%	50%	25%	75%	50%	25%
Bal	7.98	7.89	7.85	8.00	7.89	7.88	8.01	7.92	7.89
TBA-Thione	8.17	7.11	6.05	8.02	6.95	6.12	8.06	6.98	6.09
TBA-Thiol	8.22	8.12	7.45	8.22	8.12	7.35	8.25	8.15	7.38
TU	8.85	8.44	9.35	8.86	8.40	9.32	8.89	8.44	9.36

$$pH + log\frac{\overline{n}}{1-\overline{n}} = \log K_1\,,\ \overline{n} < 1 \tag{6}$$

Algebraic method has been applied to calculate the dissociation constants of ligands where the equilibrium involved as follows [50].

$$H_2A \leftrightarrow H^+ + HA^- \qquad k_1 = [H^+][HA^-]/[H_2A] \tag{7}$$

$$HA^- \leftrightarrow H^+ + A^{-2} \qquad k_2 = [H^+][A^{-2}]/[HA^-] \tag{8}$$

H_2A and parentheses represent the ligands and the molar concentrations. Since K1>K2, every dissociation stage was considered separately.
Where: C_A represents the total concentration of the ligand species and "a" represents the number of moles of base that added per mole of the ligand present. It follows of the organic co-solvent in the low pH buffer region:

$$C_A = [H_2A] + [HA^-] \tag{9}$$

$$aC_A + [H^+] = [HA^-] + [A^{2-}] \tag{10}$$

$$K_1 = \frac{[H^+](aC_A + [H^+])}{C_A - (aC_A + [H^+])} \tag{11}$$

In the high pH buffer region, the concentration of the acid from (H_2A) of the ligand is neglected and so:

$$K_2 = \frac{[H^+]((a-1)C_A - [OH^-])}{(2-a)C_A - [OH^-]} \tag{12}$$

All ligands in different percentages of ethanol-water media gave one pK's value based on potentiometric measurements indicating that different mechanisms are produced:

(1) Tautomerism produced of CH-CO skeleton.
(2) Tautomerism produced of NH-CO skeleton.
(3) Tautomerism produced of NH-CS skeleton.

The distinction within the pK value of the barbital to that of thiobarbituric skeleton because of that sulphur is less electronegative than oxygen. This makes thiobarbituric acid to be less acidic than barbital. In turn, gives higher pK value compared to barbital.

By increasing the percentage of ethanol from 25% to 50% and then to 75% gave the same trend however the curves shifted to a higher pH. These results in the pK values increase with increasing ethanol percentage due to the dielectric properties of the ethanol that decrease the dissociation of the ligand species, the higher concentration of the solvent results in ligand-ethanol interaction through hydrogen bond formation.

The potentiometric information shows that, the pK values depend on both the nature and also the proportion of the organic cosolvent. by increasing the organic cosolvent content within the medium the pK value increase. However, the acidity constants in a pure aqueous medium (Ka_1) associated with that in water-organic solvent mixtures (Ka_2) by the equation [51].

$$K_{a1} = K_{a2}\left(\frac{\gamma_{H^+}\gamma_{A^-}}{\gamma_{HA}}\right) \quad (13)$$

Where: y is that the activity coefficient of the subscripted species in a partially aqueous medium to that in a pure aqueous one. Since it is illustrious that the electrostatic effects of solvents operate only on the activity coefficients of charged species [52], one will expect that the rise within the quantity of the organic co-solvent within the medium can rise the activity coefficients of both H^+ and A^- ions. This can lead to a decrease in the acid dissociation constant (high pK value), that is consistent in keeping with the results obtained for the investigated compounds.

The effects of ethanol solvent on the behavior of those ligands are discussed using another scope. It was assumed that the J factor represents a solvent-transfer number characteristic of the tested chemical reaction that can be attributed to the transfer of the solvent. The subsequent equation is tested [53-54].

$$J \log [S] - \log K = -\Delta G/(2.303\ RT) - W \log [H_2O]/[S];$$
$$\log [H_2O/S] = X; \quad J \log [S] - \log K = Y$$

Where: [S] and ΔG represent the solvent concentration and the free energy respectively. The data are collected in table 7, Trail values of J = 1, 2, 3, 4 are used to find values of W for the gradients of Y vs. X (the slopes give the values of water molecules (W)). The data obtained may throw light on the role of equation and solvation during the dissociation, where the solute molecules are surrounded by water and solvent molecules in different manner. This in fact can`t, however, tell much about the nature of association between solute species and solvent molecules, whether the value of J is due to only the molecules in the primary solvation zone or includes molecules external to but closely associated with these.

For all ligands at different percentages of ethanol- Water mixture, the (W) values for J=I, 2, 3, 4 at 25°C are lower than that of J values to pinpoint more solvation. At TU the pK_1 at J=1 the equation and solvation are coexists due to $W \approx J$.[54]

3.4 Complex formation studies

By scrutiny the pH titration curves of the free ligands thereto of the complex solutions, drop of the pH values occurs suggesting that the mechanism of complexation relies on proton liberation. An advantage was taken of the features of this curves ion (i) the Preliminary assessment of the complex stoichiometric, (ii) the final choice of the “best" set of formation constants for the system, based on graphical comparisons as developed above. In the calculation of the stability constants, it was assumed that factors like hydrolysis of metal ions and therefore the presence of nuclear hydrogen and hydroxyl bearing complexes was absent and could be neglected. This might be achieved by taking low concentration of the metal ion.

No side reactions between the metal and also the anionic part of the ligand take place. The metal ion complexing will not have an effect on the relative stability values and this factor becomes common throughout. The formation of ion-pair between the anionic species and the positive part of the strong electrolyte could be neglected by controlling the ionic strength of the solution, to be of low values. The activity coefficients of all species were constant. So, the concentration term may well be used rather than activities.

Table 7. X-Y data in different percentages of ethanol-water media at 25°C for variable values of (J)

	Y at 25°C						
Ligand	[s], %	log[s]	-X	J=1	J=2	J=3	J=4
Bal	25	1.398	-0.477	9.378	10.776	12.174	13.572
	50	1.699	0	9.589	11.288	12.987	14.686
	75	1.875	0.477	9.725	11.600	13.475	15.350
TBA-Thione	25	1.398	-0.477	9.568	10.966	12.364	13.762
	50	1.699	0	8.809	10.508	12.207	13.906
	75	1.875	0.477	7.925	9.800	11.675	13.550
TBA-Thiol	25	1.398	-0.477	9.618	11.016	12.414	13.812
	50	1.699	0	9.814	11.513	13.212	14.911
	75	1.875	0.477	9.325	11.200	13.075	14.950
TU	25	1.398	-0.477	10.248	11.646	13.044	14.442
	50	1.699	0	10.139	11.838	13.537	15.236
	75	1.875	0.477	11.225	13.100	14.975	16.850

The acid-base properties of the free ligands facilitate the investigation of the coordinating behavior of those ligands towards Zr(IV). It is apparent that the ligands under investigation have strong coordinating ability. The pK values of the free ligands have been affected by complexation. The free ligand exponent pL, the degree of formation of the system n and hence the stability constants of the metal ligand complexes could be calculated by the measurements during titration of the solution of chelating agent in the presence and in absence of metal ions with alkali could, Where C_M and C_L represent the analytical concentrations of the metal and ligand, respectively. Plotting the $\bar{n}$ values against pL, values at $\bar{n}$ equals to 0.5 [48], table 8, give the corresponding pK values.

Concordant results have been obtained on applying the point-wise calculation method [49]. On plotting log $\bar{n}$ function against pL, straight lines are obtained from that log K values are obtained. table 8 shows the log K and stoichiometry of the complexes at 25°C.

Table 8. Stability constants of Zr(IV) complexes with ligands at 25°C

Ligand	$\bar{n}_A$ - pL			Point-wise method		
	75%	50%	25%	75%	50%	25%
Bal	7.59	7.04	6.41	7.58	7.00	6.42
TBA-Thione	7.94	6.65	6.25	7.93	6.66	6.31
TBA-Thiol	9.30	8.90	9.45	9.28	8.91	9.48
TU	7.83	7.54	7.08	7.86	7.55	7.09

Different values of the stability constants of the complexes are obtained in different concentrations of the complex species. The concentration distribution of various (Bal, TBA-thione, TBA-thiol and

TU) and their complexes species in solution as a function of pH were calculated and plotted by applying SPE and SPEPLOT computer programs [55], figures 11and12.

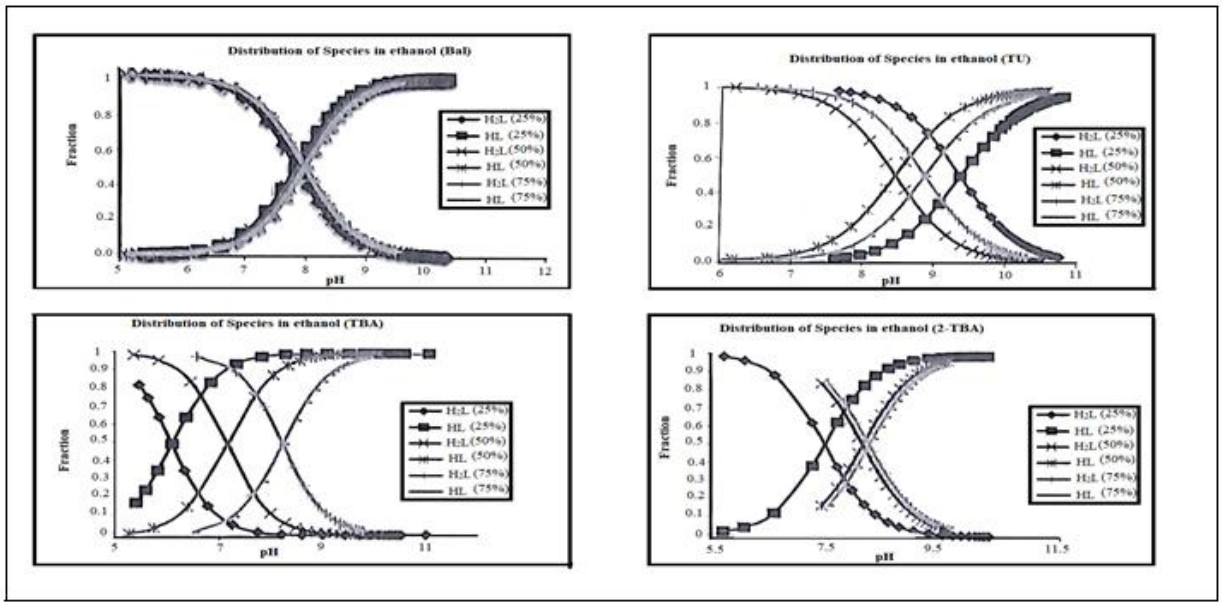

Figure 11. Distribution of species diagram of the ligands.

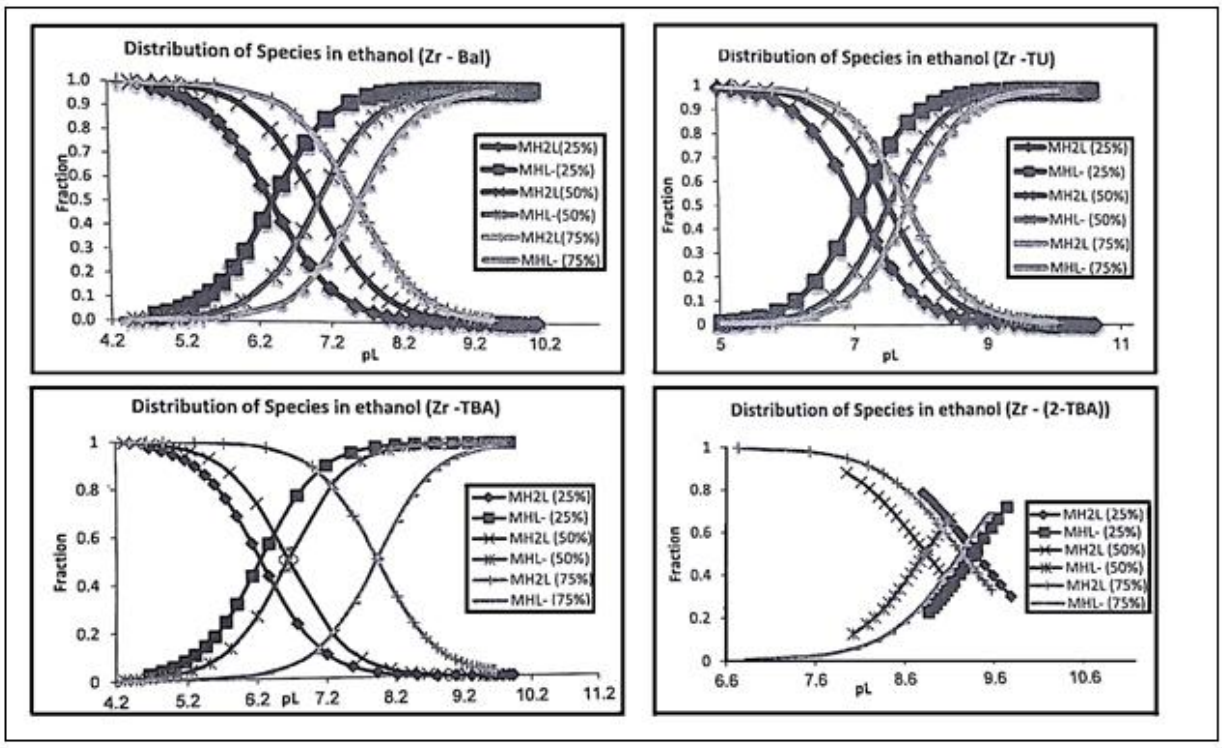

Figure 12. Distribution of species diagram of the complexes.

From the plotting of the ligand species fraction and the pH in different % ethanol, depending on the pK values, one can give the following points:

1. For Bal, the curves start with high % of [HL] species which decreased with increasing pH with appearance of [HL] species at pH around 5.09. The concentration of both [H_2L] and HL seems to be the same i.e. each with 0.5 fractions. With increasing pH the HL^- predominates till reach a maximum fraction at pH= 10.
2. For TU, the curves start with high % of [H_2L] species which decreased with increasing pH with appearance of [HL] species at pH around 6.19. The concentration of both [H_2L] and [HL^-] seems to be the same i.e. each with o.5 fraction, with increasing pH the [HL^-] predominates till reach a maximum fraction at pH=10.5.
3. For TBA- thione, the curves start with high % of [H_2L] species which decreased with increasing pH with appearance of HL species at pH around 5.63. The concentration of both [H_2L] and [HL^-] seems to be the Same i.e. each with 0.5 fraction, with increasing pH the [HL^-] predominates till reach a maximum fraction at pH 10.5.
4. For TBA-thiol, the curves start with high % of [H_2L] species which decreased with increasing pH with appearance of [HL^-] species at pH around 6.5. The concentration of both [H_2L] and [HL^-] seems to be the same i.e. each with 0.5 fraction, with increasing pH the [HL^-] predominates till reach a maximum fraction at pH=10.
5. By increasing the % of ethanol from 25% to 50% and then to 75% gave the same trend but the curves shifted to a higher pH. This leads to the fact that the pK values increase with increasing ethanol %, and this may be due to the dielectric properties of the ethanol that retard the dissociation of the ligand species.
6. On comparing the TBA with 2-TBA in (75% and 50% ethanol - water), it showed that the species distribution curves for TBA takes apart more than 2-TBA in case of HL -(2-TBA) at lower fraction and higher apparent pH vales. Meanwhile, the distribution of species in (75%, 50% and 25% ethanol -water) TBA and 2-TBA complexes show the same trend.
7. The study of the Zr-Bal complexes gave the same trend for the free ligand, where on increasing pH the existence of the [MH_2L] species decreased to a minimum at pH 9 while the [MHL^-] species Starts to increase in the pH range 4.29 -9 then predominates.
8. The study of the Zr- TU complexes gave the same trend for the free ligand, where on increasing pH the existence of the [MH_2L] species decreased to a minimum at pH =9 while the [MHL-] species starts to increases in the pH range 5.12-9 then predominate.
9. The study of the Zr-TBA complexes gave the same trend for the free ligand, where on increasing pH the existence of the [MH_2L] species decreased to a minimum at pH= 9.5 while the [MHL^-] species starts to increase in the pH range 4.2-9.5 then predominate.
10. The study of the Zr-2TBA complexes gave the same trend for the free ligand, where on increasing pH the existence of the [MH_2L] species decreased to a minimum at pH=9.5 while the [MHL^-] species starts to increase in the pH range 8-9.5.

4. Conclusion

- The infra-red spectra assigned the different modes of vibrations of the fundamental functional groups. The measurements referred that barbituric acid, thiouracil and barbital exist in the keto form, thiobarbituric acid is in keto and enol form.
- The change in entropy values, $\Delta S^{\#}$, for all complexes lie within the range -0.267, -0.299 $KJK^{-1}\,mol^{-1}$.
- The thermal processes proceed in complicated mechanisms with more ordered transition states.
- The DSC studies shows that the crystallization temperatures (T_c) of the complexes studied were around 78◦C – 322.12◦C.
- The stability constant for Zr(IV) with barbital was from (6.41-7.59), with thiobarbituric acid-thione (6.25-7.94), with thiobarbituric acid-thiol (8.90-9.45) and for Thiouracil (7.08-7.83) at different percentages of ethanol.

5. References

[1] Hueso-Urena F, Illan-Cabeza N A, Moereno-Carretero M N, Martinez-Matose J M and Ramirez-exposito M J, 2003 *J. Inorg. Biochem 94*, 326-334.
[2] Refat M S, El-Korashy S A and Ahmed A S, 2008 *Spectochim. Acta A, 71*, 1084-1094.
[3] Tsunoda A, Shibisawa M, Yasuda Y and Nakao N, 1994 *Anticancer Res. 14*, 2637-2642.
[4] Casas J S, Castellans E E, Louce M D, Ellena J, Sanchez A, Sordo J and Taboada C,*2006 J. Inorg. Biochem , 100*, 11, 1858-1860.
[5] Campbell M J, 1975 *Chem. Rev. 15*, 279-319.
[6] Masoud M S, Khalil E A, Ramadan A M, Gohar Y M and Sweyllam A, *2007 Spectrochim Acta A, 67*, 669-677.
[7] Masoud M S, Awad M K, Shaker M A and El-Tahawy M M T, 2010 *Corros. Sci. 52*, 2387-2396.
[8] Uhlmann C, Fröscher W and Neurosci CNS. 2009 *Ther. 15*, 24-31.
[9] Sokmen B, Ugras S, Sarikaya H, Ugras H and Yanardag R, 2013 *App Bio. Biotech, 171*, 2030-2039
[10] Ma L, Li S, Zheng H, Chen J, Lin L, Ye X, Chen Z, Xu Q, Chen T, Yang J, Qiu N, Wang G, Peng A, Ding Y, Wei Y and Chen L, 2011 *Eur. J. Med. Chem. 46*, 2003-2010.
[11] Uciechowska U, Schemies J, Neugebauer R C, Huda E M, Schmitt M L, Meier R, Verdin E, Jung M and Sippl W, 2008 *Chem. Med. Chem. 3*, 1965-1976.
[12] Maquoi E, Sounni N E, Devy L, Olivier F, Frankenne F, Krell H W, Grams F and Foidart J M, 2004 *Clin. Cancer Res. 10*, 12, 4038-4047.
[13] Xia G, Benmohamed R, Kim J, Arvanites A C, Morimoto R I, Ferrante R J, Kirsch D R and Silverman R B,2011 *J. Med. Chem. 54*, 2409-2421.
[14] McCluskey A J, Robinson P, Tim H, Janet L, Scott C and Edwards A K, 2002 *Tetrahedron Lett. 43*, 3117-3120.
[15] Kadoma Y and Fujisawa S, 2012 *Polymers, 4*,2, 1025-1036.
[16] Langer M, Kratz F, Rothen-Rutishauser B, Wunderli-Allenspach H and Beck-Sickinger A G, 2001 *J. Med. Chem.44*, 1341-1348.
[17] Alyar S and Karacan N, 2009 J. Enzyme Inhib. *Med. Chem.* 24, 986-992.
[18] Fathalla A, Zaghary W A, Radwan H H, Awad S M and Mohamed M S, 2002 *Arch. Pharm. Res.* 25, 3, 258-269.
[19] Awad S M, Zohny Y M, Ali S A, S. Mahgoub and Said A M, 2018 *Molecules, 23*, 11, 2913-2926.
[20] Cotton F A, Wilkinson G and Gaus P L, 1995 Basic Inorganic Chemistry, 3th ed. John Wiley & Sons, Inc.: Singapore.
[21] Blumenthal W B, 1962 *J. Chem. Educ. 39*, 604–610.
[22] Blumenthal W B, 1968 *Talanta, 15*, 877–882.
[23] Blumenthal W B, 1973 *Am. Ind. Hyg. Assoc. J. 34*, 128–133.
[24] Nikunj B B, Darpan N P and Thaddeus J W, 2018 *Molecules, 23*,3, 638-641.
[25] Kuhlmann L, Methling R, Simon J, Neumann B, Stammler H G, Strassert C A and Mitzel N, 2018 *Dalton Transactions*, 47, 11245-11252.
[26] a) Baldo M A, O'Brien D F, You Y, Shoustikov A, Sibley S, Thompson M E and Forrest S R, 1998 *Nature, 395*, 151-154.; b) Sajoto T, Djurovich P I, Tamayo A B, Oxgaard J, Goddard W A and Thompson M E, 2009 *J. Am. Chem. Soc. 131*, 28, 9813-9822.
[27] Kober E M, Caspar J V, Lumpkin R S and Meyer T J, 1986 *J. Phys. Chem. 90*, 16, 3722-3734.
[28] Sanning J, Ewen P R, Stegemann L, Schmidt J, Daniliuc C G, Koch T, Doltsinis N L, Wegner D and Strassert C A, 2015 *Angew. Chem. Int. Ed. 543*, 786-791.
[29] Lubczak J and Lubczak R, 2018 *Int. J. Chem. Kinetics, 50*,2, 122-132
[30] Masoud M S, Soayed A A and Ali A E, 2004 *Spectrochim. Acta A, 60*, 1907-1915.

[31] Masoud M S, Haggag S S and Khalil E A, 2006 *Nucleosides, Nucleotides and Nucleic Acids*, *25*, 1, 73-87.
[32] Masoud M S, Hindawy A M, Soayed A A and Abd El-Kaway M Y, 2011 *J. Fluid Phase Equilibria*, *312*, 37-59.
[33] Masoud M S, Abd El-Kaway M Y, Hindawy A M and Soayed A A, 2012 *Spectrochimica Acta Part A*, *92*, 256-282.
[34] Masoud M S, Ramadan A M and El-Ashry Gh M, 2013 *Thermo Chimica Act*, *551*, 164-174.
[35] Masoud M S and Abd El-Kaway M Y, 2013 *Spectro Chim. Acta A*, *102*, 175-185.
[36] Masoud M S, Awad M K, Shaker M A, Ali A E and El-Tahawy M, 2013 *Research on Chemical Intermediates*, 6, 2741-2761.
[37] Masoud M S, El-Marghany A, Orabi A, Ali A E and Sayed R, 2013 *Spectrochimica Acta A, 107*, 179-187
[38] Masoud M S, Ali A E and Abd El-Kaway M Y, 2014 *J. Thermal Analysis and Calorimetry*, *116*, 183-194.
[39] Masoud M S, Kamel H M and Ali A E, 2015 *Spectrochim. Acta A*, *137*, 1417-1425.
[40] Masoud M S, Elsamra R M I and Hemdan S S,2017 *J. Serb. Chem. Soc*. *82*,7-8, 851-864.
[41] Gelsema W J, Deltgny C L , Remijnse A G and Bluleven H A, 1966 *Recueil* **,** *85*, 647-659.
[42] Foye W O, Lemke T L and Williams D A, 1995 *Principles of Med. Chem*., 4th ed. Williams & Wilkins, Philadelphia, *88*, 89, 154-180.
[43] Bolton W, 1963 *Acta cryst. 16*, 166-173.
[44] Price W C, Bradley J E S, Fraser R D B and Quilliam J P, 1954 *J. pharm. and Pharmacol. 6*, 522-528.
[45] Wills Jr. J N, Cook R B and Jankow R,1972 *Anal. Chem*. *44*, 1228-1234.
[46] Mesley R J,1970 *Spectrochim. Acta A , 26*, 1427-1448.
[47] Bult A and Klasen H B,*1976 Lett.* 9, *2*, 81-94.
[48] Irving H and Rosstti H, 1953 *J. Chem. Soc.* 3397-3405.
[49] Jahagirdar D V and Khanolkar D D, 1973 *J. Inorg. Nucl. Chem*. *35*, 3, 921-930.
[50] Charberk S and Martell A E,1952 *J. Am. Chem. Soc. 74*, 20, 5052-5056.
[51] Coetzee J F and Ritchie C D, 1969*Solute- Solvent Interactions*; Marcel Dekker: New York, 221.
[52] Denison J Tand Ramsey J B, 1955 *J. Am. Chem. Soc*. *77*,9, 2615-2621.
[53] Mui K, McBryde W A E and Neiboer E,1974 *Can. J. Chem*. *52*, 10, 1821-1833.
[54] Masoud M S and Abdullah A A, 1982 *J. Chem. Eng. Data***,** *27*,1, 60-62.
[55] Martell A E and Mutekaities R J,1992 *Determination and Use of Stability Constant*, VCH, New York.